Anisotropic excitation behavior from hybridization-mediated exchange in CeBi

P. Thayamballi, D. Yang,* and Bernard R. Cooper
Department of Physics, West Virginia University, P.O. Box 6023, Morgantown, West Virginia 26506-6023
(Received 11 October 1983)

The excitation spectrum of CeBi in the type-I antiferromagnetic phase, as measured by Rossat-Mignod *et al.* using neutron scattering, is quite unusual. The excitations with wave vector $\vec{q}$ perpendicular to the ferromagnetic (001) planes are dispersionless (with an energy of about 1 THz=48 K); whereas for a wave vector within the (001) plane, a dispersion has been found with a minimum in energy at the zone boundary. The equilibrium behavior of CeBi has been explained previously by Siemann and Cooper using an interionic interaction arising from band-f electron hybridization (Coqblin-Schrieffer interaction) as mediated by band electrons. Using the same theory, calculations of the excitation spectrum are reported in the present paper. These calculations give results that compare well with the experimental excitation behavior on using a set of parameters giving equilibrium behavior similar to experiment.

I. INTRODUCTION

The NaCl-structure compounds, CeBi and CeSb, have peculiar magnetic properties which have been understood as arising through hybridization of the moderately delocalized cerium f levels with band electrons of non-f atomic parentage.[1,2] These compounds show magnetic structures with strongly ferromagnetic {001} planes, with moments perpendicular to the planes, and weak coupling between planes. This permits a variety of structures depending on the relative (up or down) moment directions between adjacent planes, and these structures can occur in a relatively small range of temperature and external magnetic field.[3] At zero field, CeBi has a low-temperature $++--$ type-IA antiferromagnetic phase which undergoes a first-order transition to a $+-$ type-I antiferromagnetic phase at about half the ordering temperature[4] (25 K). The existence of the low-temperature IA phase is sample dependent,[5,6] but the type-I phase always occurs.

The equilibrium behavior of CeBi has been explained[7] by a hybridization-mediated two-ion interaction of the Coqblin-Schrieffer[8] (CS) type. The interaction gives strong intraplanar coupling and a much weaker coupling between planes transverse to an (approximately saturated) moment direction. This behavior results from the fact that the magnetic ions are relatively far apart in the heavier (than nitride) rare-earth and actinide monopnictides, so that the f electrons have a modest delocalization and "sense" each others moment via a moderate amount of hybridization with the band electrons.[1] The joint hybridization of a pair of Ce^{3+} ions with the band electrons gives a piling up of charge along the interionic axis, and this determines a preference for alignment and size of orbital moment (and through spin-orbit coupling, the total moment) favoring saturated moments perpendicular to the interionic axis. (This involves an energy that is modest compared to the cohesive energy of the crystal, but large on the scale of magnetic ordering energies.) Compromise forced by the difference directions of interionic axis may lead to complex magnetic structures and unsaturated moments. For a fairly broad range of the ratio of ferromagnetic nearest-neighbor (NN) to next-nearest-neighbor (NNN) Coqblin-Schrieffer two-ion interaction near $E_2/E_1=1$ (in the notation of Refs. 1 and 7), the lattice geometry strongly favors magnetic structures with the basic units being {001} ferromagnetic planes with a variety of parallel or antiparallel planar moment stackings.[1]

In this paper, we further substantiate the experimental relevance of the hybridization-mediated interaction by studying the excitation behavior of the ferromagnet and the type-I antiferromagnet with equal ferromagnetic NN and NNN Coqblin-Schrieffer two-ion interaction ($E_1=E_2$), where a small NN antiferromagnetic Heisenberg interaction H_1 (the physical origin of which lies in the ordinary isotropic Ruderman-Kittel effects) stabilizes the antiferromagnetic type-I phase. The excitation behavior for the $E_1=E_2$ case has been treated in order to correspond to the experimental situation[6] where the CeBi sample studied showed only a type-I structure. For slightly larger E_2, say $E_2=1.1E_1$, and appropriate H_1, the model reproduces the $++--$ (IA) to $+-$ (I) phase transition.[7]

We have compared our results with the experimental excitation behavior[6] of a CeBi sample which showed only a type-I antiferromagnetic structure. Our theory agrees well with experiment, reproducing the dispersionless mode for $\vec{q}$ along [001] (the direction of moment and of propagation vector of the magnetic structures) and the minimum in energy at the zone boundary $X(2\pi/a,0,0)$ for $\vec{q}$ along the [100] direction. Such behavior was not obtained by Rossat-Mignod *et al.*[6] when they tried to reproduce their experimental behavior with a Heisenberg exchange model which assumes one set of NN and NNN coupling constants within the ferromagnetic (001) planes and another set of NN and NNN coupling constants between planes.

II. METHOD OF CALCULATION

The hybridization-mediated interaction Hamiltonian, in its Fourier-transformed form, can be written[1,9]

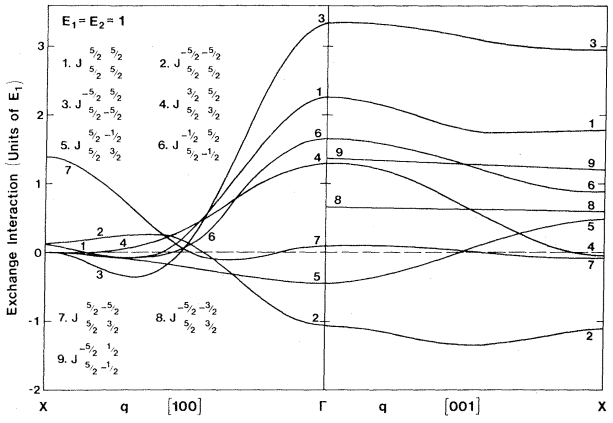

FIG. 1. The exchange coefficients $J^{\epsilon\sigma}_{\mu\nu}(\vec{q})$ [see Eq. (1)] for $\vec{q}$ along the [001] (axis of quantization and direction of moment) and [100] directions in a fcc crystal for ferromagnetic CS interactions $E_1=E_2$. The coefficients shown have $\pm\frac{5}{2}$ as at least one of the upper and lower indices (coefficients pertinent when the ground state has an almost saturated moment).

$$\mathcal{H}_{\rm CS}=-\sum_{\vec{q}}\sum_{\substack{\mu\nu\\ \epsilon\sigma}} J^{\epsilon\sigma}_{\mu\nu}(\vec{q})L^{\vec{q}}_{\mu\nu}L^{-\vec{q}}_{\epsilon\sigma}\ , \tag{1}$$

where we use greek letters to label the states of the single ion by the z component M_J of the angular momentum ($J=\frac{5}{2}$) with the axis of quantization along the [001] direction in the crystal. $L^i_{\alpha\beta}=|\alpha\rangle\langle\beta|$ is an operator which takes the Ce^{3+} ion on site i from state $|\beta\rangle$ to state $|\alpha\rangle$, and L^q is the Fourier transform of L^i. The exchange coefficients $J^{\epsilon\sigma}_{\mu\nu}(\vec{q})$ depend on the CS interaction strength E_n to each of the nth nearest neighbors and the angle between each interionic axis and the axis of quantization [001]. The behavior of the $J^{\epsilon\sigma}_{\mu\nu}(\vec{q})$, with at least one upper and one lower index $=\pm\frac{5}{2}$ (pertinent for a saturated ground state), is shown in Fig. 1 for equal ferromagnetic NN and NNN CS interactions between $Ce^{3+}(J=\frac{5}{2})$ ions on a fcc lattice. The relative flatness of curves 1 and 2 for $\vec{q}$ along [001] corresponds to the weak coupling between (001) planes in the equilibrium state when the moments are close to saturation along [001]. The smaller dispersion along [001] compared to that along [100] for curves 3–9 will be reflected in the excitation behavior discussed below.

The equilibrium behavior of the system is found by diagonalizing the interaction Hamiltonian in the molecular field (MF) approximation. [Besides the CS two-ion interaction, the interaction Hamiltonian may contain Heisenberg interactions, which can again be cast in the form of Eq. (1), and there may also be additional single-ion terms coming from the crystal field and external magnetic fields, which can easily be taken into account.] To study the excitations of the system, we project the Hamiltonian into the MF manifold:[9]

$$\mathcal{H}=\mathcal{H}_{\rm MF}+\mathcal{H}'\ , \tag{2}$$

$$\mathcal{H}_{\rm MF}=\sum_i\sum_m \mathscr{E}^i_m L^i_{mm}\ , \tag{3}$$

$$\mathcal{H}'=-\sum_q\sum_{\substack{\mu\nu\\ \epsilon\sigma}} J^{\epsilon\sigma}_{\mu\nu}(\vec{q})(L^{\vec{q}}_{\mu\nu}-\langle L^{\vec{q}}_{\mu\nu}\rangle)(L^{-\vec{q}}_{\epsilon\sigma}-\langle L^{-\vec{q}}_{\epsilon\sigma}\rangle)\ , \tag{4}$$

where we have denoted the MF states in Eq. (3) by lowercase latin letters, and $\mathscr{E}^i_m$ denotes the energy of the MF state $|m\rangle$ on site i. Equation (3) for $\mathcal{H}_{\rm MF}$ is obtained by diagonalizing the MF Hamiltonian [which is the difference of Eqs. (1) and (4)]. The Hamiltonian $\mathcal{H}'$ of Eq. (4) induces transitions between MF states. The only nonzero expectation values $\langle L^{\vec{q}}\rangle$ are obtained for $\vec{q}$ characteristic of the equilibrium magnetic structure [e.g., $\vec{q}=0$ for a ferromagnet, and $\vec{q}=0$ and $(2\pi/a)(0,0,1)$ for a collinear type-I antiferromagnet].

To transform $\mathcal{H}'$ to the MF basis we use the transformation obtained by diagonalizing the MF Hamiltonian:

$$|m\rangle_i=X^i_{m\mu}|\mu\rangle\ , \tag{5}$$

where i denotes the ionic sites. The coefficients $X_{m\mu}$ for some of the cases we have investigated are shown at the right in Figs. 2–6. For the type-I antiferromagnet, the $X_{m\mu}$ shown are for the up sublattice; those for the down sublattice are obtained by time reversal.

To find the excitations at $T=0$, we need only consider the set of operators that take the system from, or to, the MF ground state (L_{n1} or L_{1n}). The dynamics of the system is found by using the equation-of-motion technique. For a system with equal MF energies on all sites, the commutators with the MF Hamiltonian are

$$[\mathcal{H}_{\rm MF},L^{\vec{q}}_{mn}]=(\mathscr{E}_m-\mathscr{E}_n)L^{\vec{q}}_{mn}\ . \tag{6}$$

In calculating the commutator with $\mathcal{H}'$ we use the random-phase approximation (RPA) to decouple terms with more than one L_{mn} operator. For the case of a ferromagnet this yields

$$[\mathcal{H}',L^q_{mn}]=2(\langle L^0_{mm}\rangle-\langle L^0_{nn}\rangle)\sum_{rs}J^{rs}_{nm}(\vec{q})L^{\vec{q}}_{rs}\ . \tag{7}$$

The thermal average $\langle L^0_{mm}\rangle$ is unity if m is the ground state ($m=1$), and zero otherwise. The resulting dynamical matrix is 10×10 (upwards and downwards transitions between the ground state and each of the five molecular field excited states), and on diagonalizing, it gives five modes at energy gain and five at energy loss.

In the case of a type-I structure, the equations of motion involve a mixture of motions on both the sublattices. For a system with equal MF energies on both sublattices and states on the two sublattices being time-reversed states of each other (i.e., a conventional two-sublattice antiferromagnet), we obtain the result

$$[\mathcal{H}',L^{\vec{q}}_{mn}]=2(\langle L^0_{mm}\rangle-\langle L^0_{nn}\rangle)\sum_{rs}\sum_{\substack{\mu\nu\\ \epsilon\sigma}}\{[J^{\epsilon\sigma}_{\mu\nu}(\vec{q})\alpha^{nm}_{\mu\nu}\alpha^{rs}_{\epsilon\sigma}+J^{\epsilon\sigma}_{\mu\nu}(\vec{q}+\vec{Q})\beta^{nm}_{\mu\nu}\beta^{rs}_{\epsilon\sigma}]L^{\vec{q}}_{rs}$$
$$+[J^{\epsilon\sigma}_{\mu\nu}(\vec{q})\alpha^{nm}_{\mu\nu}\beta^{rs}_{\epsilon\sigma}+J^{\epsilon\sigma}_{\mu\nu}(\vec{q}+\vec{Q})\beta^{nm}_{\mu\nu}\alpha^{rs}_{\epsilon\sigma}]L^{\vec{q}+\vec{Q}}_{rs}\}\ , \tag{8}$$

where $J^{\epsilon\sigma}_{\mu\nu}$ are given in Eq. (4), $\vec{Q}$ [$=(2\pi/a)(0,0,1)$] is the propagation vector of the type-I antiferromagnetic structure, and m,n,r,s label the MF states in order of increasing energy. α and β are defined by

$$\alpha^{mn}_{\mu\nu}=\tfrac{1}{2}(X^{\mathrm{I}*}_{m\mu}X^{\mathrm{I}}_{n\nu}+X^{\mathrm{II}*}_{m\mu}X^{\mathrm{II}}_{n\nu})\ , \tag{9a}$$

$$\beta^{nm}_{\mu\nu}=\tfrac{1}{2}(X^{\mathrm{I}*}_{m\mu}X^{\mathrm{I}}_{n\nu}-X^{\mathrm{II}*}_{m\mu}X^{\mathrm{II}}_{n\nu})\ , \tag{9b}$$

where I and II refer to the up and down sublattices. The MF transformation coefficients $X^{i}_{m\mu}$ are defined by Eq. (5), and the asterisk denotes complex conjugation. (For the type-I structure considered here, the coefficients are real.) Equations (8) and (9) clearly show the mixing between the two sublattices. These equations lead to a 20×20 matrix which has to be solved to find the correlated motion of the sublattices.

We are interested in the linear response of the system to an oscillating magnetic field, or to propagating neutrons. Of all possible matrix elements of the angular momentum operators J_z, J_+, J_- between the molecular field ground state and the excited states, the largest matrix element is found for the 1 to 4 (or 4 to 1) transition of Figs. 2–4 and the 13 (or 31) transition of Figs. 5 and 6. (In all the figures, the MF states are labeled in order of increasing energy.) This strength comes from the $M_J=\frac{5}{2}$ to $\frac{3}{2}$ transverse transition. (The MF ground state is predominantly $|\frac{5}{2}\rangle$.) All the other matrix elements between ground and excited MF states are at least an order of magnitude smaller; therefore, we shall only be concerned with this intense transverse transition.

Since, in general, the normal modes of the system are made up of a mixture of all the L_{1n} and L_{n1} modes, the intensity of any normal mode depends on how much of L_{14} and/or L_{41} is present in it. *The solid curves in the figures show the intense modes which are likely to be observed experimentally.* As $\vec{q}$ varies, the total spectral weight is a constant, and when more than one mode is shown as being intense at the same $\vec{q}$ point, the intensity of any one of these modes is at least $\frac{1}{3}$ of that of the most intense mode. As we follow an intense mode along a $\vec{q}$ direction, if the intensity divides from one mode to more than one mode, the intensity of the originally intense single mode reduces gradually, while the newer branches pick up the difference. [Sometimes, as in Figs. 2 and 3, we obtain a soft mode, but this may be an artifact of the RPA. Furthermore, these soft modes do not contain the L_{41} (or L_{14}) transition and so they are not appreciable in intensity away from $\mathscr{E}=0$. Thus a soft mode, such as L_{61} in Fig. 2 or L_{51} in Fig. 3, has a large intensity when its energy is close to zero, but rapidly loses intensity as its energy becomes different from zero.]

Along a general direction in $\vec{q}$ space the normal modes can be made up of a mixture of all the transitions given by the L_{1n} and L_{n1}. However, at special $\vec{q}$ points, and along directions of high symmetry, there is a decoupling of modes of different characters. For the cube edge directions investigated here, the excitations along the moment direction (longitudinal) and perpendicular to it (transverse) are decoupled. The 1 to 3 transition is longitudinal and the 1 to 2 transition is a quadrupolar excitation; the 14, 15, and 16 transitions are transverse. (In Figs. 5 and 6, because of the reordering of MF energies as H_1 increases, 13 is transverse and 14 is longitudinal.) As discussed above, the transverse modes contain the intense 14 transition, and hence these are of primary interest to us. For $\vec{q}$ along the cube edge directions in the ferromagnet the transverse normal modes are found by diagonalizing the following 6×6 matrix:

$$\begin{pmatrix}
\mathscr{E}_{14}+2J^{14}_{41} & 2J^{15}_{41} & 2J^{16}_{41} & 2J^{41}_{41} & 2J^{51}_{41} & 2J^{61}_{41} \\
2J^{14}_{51} & \mathscr{E}_{15}+2J^{15}_{51} & 2J^{16}_{51} & 2J^{41}_{51} & 2J^{51}_{51} & 2J^{61}_{51} \\
2J^{14}_{61} & 2J^{15}_{61} & \mathscr{E}_{16}+2J^{16}_{61} & 2J^{41}_{61} & 2J^{51}_{61} & 2J^{61}_{61} \\
-2J^{14}_{14} & -2J^{15}_{14} & -2J^{16}_{14} & \mathscr{E}_{41}-2J^{41}_{14} & -2J^{51}_{14} & -2J^{61}_{14} \\
-2J^{14}_{15} & -2J^{15}_{15} & -2J^{16}_{15} & -2J^{41}_{15} & \mathscr{E}_{51}-2J^{51}_{15} & -2J^{61}_{15} \\
-2J^{14}_{16} & -2J^{15}_{16} & -2J^{16}_{16} & -2J^{41}_{16} & -2J^{51}_{16} & \mathscr{E}_{61}-2J^{61}_{16}
\end{pmatrix}\ , \tag{10}$$

where $\mathscr{E}_{mn}=\mathscr{E}_m-\mathscr{E}_n$ and the J^{rs}_{mn} depend on $\vec{q}$. The elements of this matrix follow from Eqs. (6) and (7) when m (or n)$=1$ and n (or m)$=4,5,6$.

An idea of the behavior of the exchange coefficients J^{rs}_{mn} in the molecular field basis can be obtained from the $J^{\epsilon\sigma}_{\mu\nu}$ (where μ, ν, ϵ, σ give the M_J quantum number for quantization along [001]), by neglecting terms to second order in the small (mixing) M_J terms present in these MF states. The relations between some of the exchange coefficients in the two basis sets are given below for the $E_1=E_2=|E_1|$, $H_1=-0.0217E_1$ ferromagnet (refer to Fig. 2 for specification of the MF states). For the other cases to be discussed, these relations may be modified, both due to the change in the order of the MF levels, and due to changes in the numerical factors in (f) and (g) of Eqs. (11) which follow:

$$\begin{aligned}
&\text{(a) } J^{41}_{14}\simeq J^{3/2,5/2}_{5/2,3/2},\ \text{(b) } J^{51}_{15}\simeq J^{-1/2,5/2}_{5/2,-1/2}\ ,\\
&\text{(c) } J^{61}_{16}\simeq J^{-5/2,5/2}_{5/2,-5/2},\ \text{(d) } J^{15}_{14}\simeq J^{5/2,-1/2}_{5/2,3/2}\ ,\\
&\text{(e) } J^{16}_{14}\simeq J^{5/2,-5/2}_{5/2,3/2},\ \text{(f) } J^{16}_{15}\simeq 0.14J^{5/2,3/2}_{5/2,-1/2}\ ,\\
&\text{(g) } J^{61}_{14}\simeq 0.14J^{3/2,5/2}_{5/2,3/2}-0.14J^{-5/2,5/2}_{5/2,-5/2}\ .
\end{aligned} \tag{11}$$

The exchange coefficients on the right in these equations (in the M_J along [001] representation) are shown in Fig. 1 for $\vec{q}$ along the [001] and [100] directions. Their behavior will enter into our understanding of the shapes of the dispersion curves for the transverse excitations as discussed below.

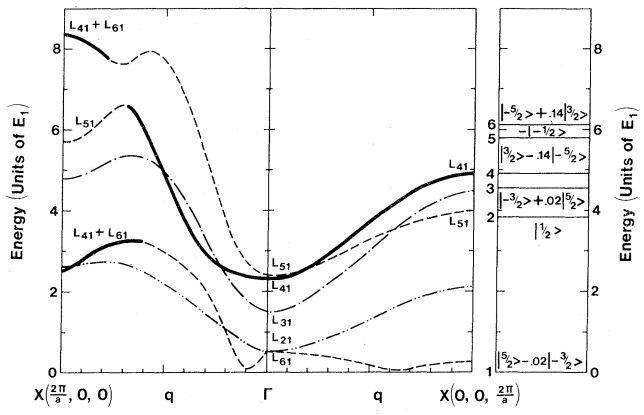

FIG. 2. Dispersion curves for the excitations at $T=0$ for the ferromagnet with CS two-ion interaction and a value of Heisenberg interaction H_1 ($=-0.0217E_1$) such that the energies of the ferromagnet and the type-I antiferromagnet are equal at zero temperature, for $\vec{q}$ along [100] and [001] (parallel and transverse to the moments). The solid curves show the most intense modes (those that are likely to be observed experimentally). The solid (——) and dashed curves (— — —) indicate excitations transverse to the moment direction. The —·— curve is that for longitudinal excitations and the —···— curve is for quadrupolar excitations. The mean field (MF) states are shown on the right-hand side in each figure; the modes L_{mn} are labeled by the corresponding dominant transition between these MF levels. This labeling of curves and modes is used in the remaining figures.

III. DISCUSSION OF RESULTS

For a system of Ce^{3+} ions on a fcc lattice, where the only interactions present are ferromagnetic CS two-ion interactions $E_1=E_2=|E_1|$, the ground state is an (001) ferromagnet.[1,7] For the $E_1=E_2=|E_1|$ case, by introducing a small antiferromagnetic nearest-neighbor Heisenberg interaction H_1, one causes a transition to a type-I antiferromagnet. [The Heisenberg interaction Hamiltonian is $-(H_1/12)\sum_{i\neq j}\vec{J}_i\cdot\vec{J}_j$, and the interaction constants E_1 and E_2 are as defined in Refs. 1, 7, and 9.] The free energy of the ferromagnet crosses that of the type-I antiferromagnet at $H_1=-0.0217E_1$. While several other magnetic structures also have almost equal energies at that H_1 (the energies of the $++--$, $+++-$, and $++-$ all lie within 1% of that of the ferromagnet and $+-$), for H_1 only slightly greater in magnitude, one has a situation where the type-I magnetic structure is well separated as the state of lowest free energy.

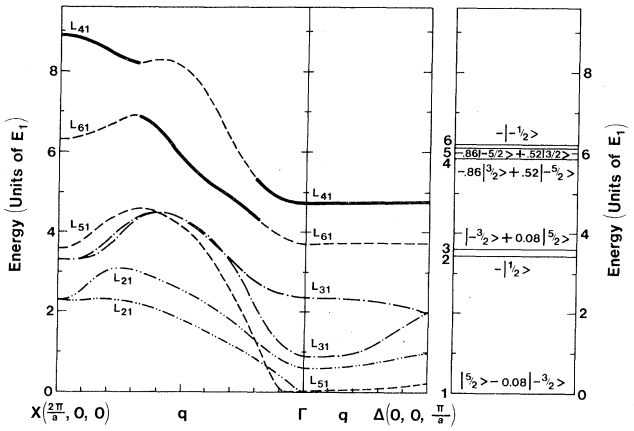

FIG. 3. Dispersion curves at $T=0$ for the type-I antiferromagnet with a value of $H_1(=-0.0217E_1)$ such that the energies of the ferromagnet and type-I antiferromagnet are equal at zero temperature.

For the ferromagnet there are only small changes in the excitation dispersion and the intensity distribution, as H_1 increases in magnitude form 0 to the critical value $-0.0217E_1$ necessary for the antiferromagnetic transition; and the spectrum is shown in Fig. 2 for the ferromagnet at the critical value of H_1. However, as shown in Fig. 3, there are major qualitative changes in both dispersion and intensity distribution upon making the transition to the type-I antiferromagnet. Further increase in the magnitude of H_1, as shown in Figs. 4–6, affects the dispersion moderately, but has a dramatic effect on the intensity distribution. We now discuss this behavior in detail. We first discuss the salient features of the spectra for the ferromagnet with $\vec{q}$ along [001] and [100], and then discuss the behavior for the type-I antiferromagnet. In particular, we shall see the effect on the excitation spectra for the type-I antiferromagnet of progressively increasing the magnitude of the NN Heisenberg interaction (H_1) for fixed CS interaction, $E_1=E_2=|E_1|$.

For $\vec{q}$ along [001] in the ferromagnet, the 6×6 matrix block of Eq. (10) separates into two 3×3 matrices, each giving the time-reversed modes of the other. The 3×3 matrix for L_{41}, L_{15}, and L_{61} has sufficiently small off-diagonal mixing, so that the energies of these modes are given approximately by the diagonal elements of the matrix of Eq. (10),

$$\mathscr{E}_{\vec{q}}(L_{mn})=\mathscr{E}_{mn}-2J^{mn}_{nm}(\vec{q})\ . \tag{12}$$

If one uses the numbers of Fig. 1, together with Eq. (11), to compare to Fig. 2 it can be seen that the above relation is indeed followed for the L_{41}, L_{51}, and L_{61} modes. The fact that the dispersion along [001] (direction of moment alignment) is less than that along [100] (considering the intense mode) indicates that the weak coupling between planes transverse to the moment direction characteristic of the CS two-ion interaction in the equilibrium state of Ce^{3+} systems, is also true to a certain extent for the excited-state behavior. (This is discussed further below.) On the other hand, significant dispersion does remain in the dominant L_{41} mode because of the $M_J=\frac{5}{2}$ and $\frac{3}{2}$ mixing as given by $J^{3/2,5/2}_{5/2,3/2}(\vec{q})$.

For $\vec{q}$ along the [100] direction in the ferromagnet of Fig. 2, the excitation behavior is very different from that for $\vec{q}$ along [001]. Here all the transverse transitions are strongly mixed. Close to the Γ point, the energies of excitations follow the simple relation of Eq. (12). However, close to the zone boundary $X(2\pi/a,0,0)$, all the exchange coefficients J^{rs}_{mn} in the 6×6 matrix of Eq. (10) are small, except J^{16}_{14} ($\simeq J^{5/2,-5/2}_{5/2,3/2}$), as can be seen from Fig. 1. Only four nondiagonal elements are appreciable in Eq. (10), and the matrix block-diagonalizes into two 2×2 matrices (one

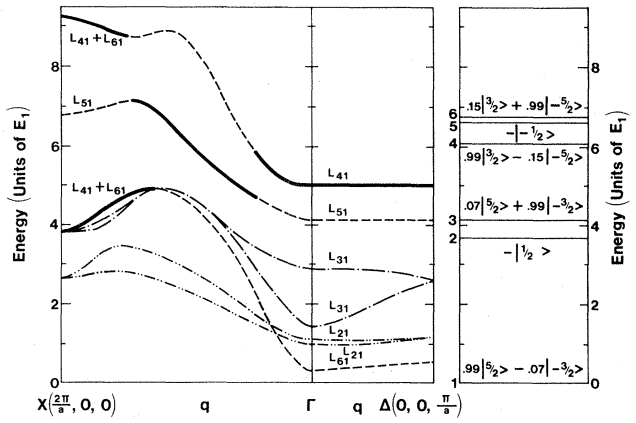

FIG. 4. Dispersion curves at $T=0$ for the type-I antiferromagnet with $E_1=E_2$, $H_1=-0.1E_1$.

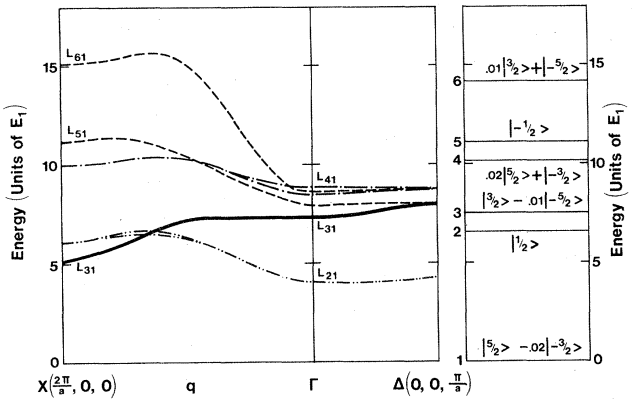

FIG. 6. Dispersion curves at $T=0$ for the type-I antiferromagnet with $E_1=E_2$, $H_1=-E_1$.

matrix couples L_{14} and L_{61}, and the other matrix is the time reversal of the first) and two 1×1 matrices (corresponding to L_{15} and L_{51}). Thus, of the three transverse modes at the band edge, the 51 mode is decoupled from the rest, with energy $\mathscr{E}_{\vec{q}}(L_{51})\simeq\mathscr{E}_{51}-2J_{15}^{51}(\vec{q})\simeq\mathscr{E}_{51}$. The strong mixing between the 14 and 61 modes through J_{14}^{16}, which increases as we get closer to the zone boundary, makes the resulting normal modes repel each other, giving a relative minimum for the low-energy mode and a relative maximum for the high-energy mode at the X point. For $E_1=E_2$ both these modes for the ferromagnet contain appreciable contributions from the L_{41} transition, and they are about equally intense. The much more pronounced rise of the 51 and 61 modes along [100] compared to that along [001] is attributed to the greater decrease of J_{51}^{15} and J_{61}^{16} for $\vec{q}$ along [100] (Fig. 1).

Turning to the type-I antiferromagnet with moments along the propagation direction [001] of the magnetic structure, we see that the excitations with $\vec{q}$ along [100] (in the ferromagnetic plane) are similar in dispersion to those along the same direction in the ferromagnet (compare Figs. 2 and 3). This is another indication that weak coupling between the ferromagnetic planes persists to at least some extent in the excitation behavior.

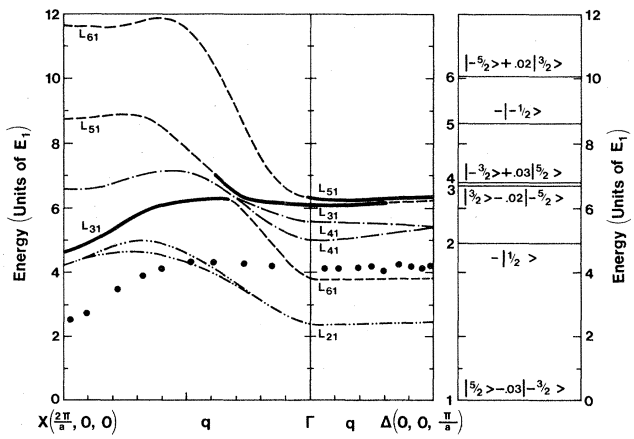

FIG. 5. Dispersion curves at $T=0$ for the type-I antiferromagnet with $E_1=E_2$, $H_1=-0.5E_1$. The experimental points of Rossat-Mignod *et al.* (Ref. 6) are shown. The scaling between experiment and theory has been made by choosing E_1 ($4E_1=1$ THz$=48$ K) to match the experimental Néel temperature ($T_N=25$ K) of CeBi.

For $\vec{q}$ along the [001] direction, the excitations in the type-I antiferromagnetic structure are markedly different from those in the ferromagnet. Here, the excitations involve combined motions of the up and down sublattices. The L_{41} mode, for example, consists predominantly of the transitions $|\frac{5}{2}\rangle$ to $|\frac{3}{2}\rangle$ on the up sublattice and $|-\frac{5}{2}\rangle$ to $|-\frac{3}{2}\rangle$ on the down sublattice (simultaneous transition of up and down sublattices toward, or away from, saturation). This is quite different from the dynamics in the ferromagnetic state where the corresponding mode involves a flip "down" (away from saturation) from $\frac{5}{2}$ to $\frac{3}{2}$ on one site and a flip "up" (toward saturation) from $\frac{3}{2}$ to $\frac{5}{2}$ on a coupled site. For the ferromagnet, the pertinent exchange coefficient giving the dispersion in mode energy is $J_{5/2,3/2}^{3/2,5/2}(\vec{q})$; while in the antiferromagnetic case, the corresponding exchange coefficient is $J_{5/2,3/2}^{-5/2,-3/2}(\vec{q})$, and this shows very little variation with $\vec{q}$ along [001]. It is the flatness of $J_{-5/2,3/2}^{-5/2,-3/2}$ for $\vec{q}$ along [001] that causes the dominant L_{41} mode to be almost dispersionless for $\vec{q}$ along [001] in the antiferromagnetic case. Similarly, the dispersion of the L_{51} and L_{61} modes are deduced from $J_{5/2,-1/2}^{-1/2,5/2}(\vec{q})$ and $J_{5/2,-5/2}^{-5/2,5/2}(\vec{q})$, respectively.

In considering the excitation behavior just described, it should be realized that weak coupling, with regard to equilibrium energy, between planes transverse to almost saturated Ce^{3+} moments does not necessarily imply correspondingly weak coupling in excited states where the system moves away from saturation. As has been discussed in Ref. 1, the weak coupling between ferromagnetic (001) planes at equilibrium corresponds to the particular distribution of charge associated with almost saturated moments pointing along [001]. The dispersionless character of the strong mode with $\vec{q}$ along [001] in the antiferromagnet means that the motion of charge associated with that mode leaves the coupling between the (001) planes totally unchanged. For the corresponding mode in the ferromagnet, this is not true.

Increasing the strength of the antiferromagnetic nearest-neighbor Heisenberg interaction H_1 in the

$E_1=E_2=|E_1|$ type-I antiferromagnet modifies the intensity distribution of the spectrum, while keeping the shape of the dispersion curves largely unchanged (Figs. 3–5). We first discuss the effects of increasing H_1 on the dispersion, and in the following paragraph discuss the effects on the intensity. For $\vec{q}$ along a cube edge direction, the effect of H_1 is to add a term of the form $4H_1[1+2\cos(qa/2)]$ to the exchange coefficients $J^{\epsilon\sigma}_{\mu\nu}(\vec{q})$ if $\mu-\nu=\sigma-\epsilon=0, \pm 1$. This changes both the MF energies and the dispersion. For $\vec{q}$ along [001], the L_{61} mode is shifted up in energy with increasing H_1 as shown in going from Fig. 4 to Figs. 5 and 6. (Since we retain the convention of numbering the MF levels in the order of increasing energy, this mode is L_{51} in Fig. 3.) We have done calculations, not included here, showing the effect for intermediate values of H_1. This shift occurs even though $J^{-5/2,5/2}_{5/2,-5/2}$ is unaffected by the Heisenberg interaction; the difference in the MF energies, $\mathscr{E}_{61}$, increases due to the presence of H_1. Hence the dispersion shape for the L_{61} mode is almost unchanged, while the mode energy increases. A similar argument applies to L_{51} (L_{61} of Fig. 3). The L_{41} mode, however, is changed both by the change in $\mathscr{E}_{41}$ and by the change in $j^{3/2\,5/2}_{5/2\,3/2}$ (which now has a term depending on H_1 and $\vec{q}$). The result is that the energy of the L_{41} mode increases faster than $\mathscr{E}_{41}$, and it gets closer to the L_{51} mode (L_{61} of Fig. 3), the energy of which differs from $\mathscr{E}_{51}$ by a constant number (as can be seen from Figs. 3 and 4), as H_1 increases for $E_1=E_2$. Also, the dispersion of the intense mode acquires a positive slope going from the Γ point toward $\Delta(0,0,\pi/a)$ point (see Figs. 5 and 6 where, because of the changes in the order of the MF levels, this mode is now labeled L_{13}).

For $\vec{q}$ along [100], important changes in relative intensity occur as H_1 increases. Of the two normal modes derived from the mixing of L_{41} and L_{61}, the lower mode increases in intensity as H_1 is increased, as compared with the upper mode. In the absence of the exchange coefficient J^{16}_{14} giving mode mixing between L_{41} and L_{61}, the lower mode is L_{41} and the upper mode is L_{61}. The Heisenberg interaction introduces additional terms in J^{14}_{41} ($\frac{5}{2}$ and $\frac{3}{2}$ mixing), while it has almost no effect on the mode-mixing term J^{16}_{14} and on J^{16}_{61} ($\frac{5}{2}$ and $-\frac{5}{2}$ mixing). Thus, as H_1 is increased, the L_{41} character of the lower branch increases, giving it larger intensity compared to the upper branch.

IV. COMPARISON WITH EXPERIMENT

It is interesting to compare the results of these calculations with the experimental excitation behavior[6] of CeBi in the type-I antiferromagnetic phase. (The sample used in the measurements of Rossat-Mignod *et al.*[6] was one where there was no transition to type-IA structure, so that the type-I behavior is pertinent at all temperatures.) The observed excitation modes for $\vec{q}$ along [001] and [100] are both transverse. The mode for $\vec{q}$ along [001] has no detectable dispersion, while the mode along [100] has a minimum at the zone boundary $X(2\pi/a,0,0)$. (See experimental points superimposed in Fig. 5.) Rossat-Mignod *et al.*[6] found that both these features cannot be simultaneously understood on the basis of a model assuming one set of NN and NNN Heisenberg exchange interactions in the ferromagnetic plane, and another set between planes. Our model does explain these results.

We obtain the dispersionless behavior for $\vec{q}$ along [001] for $E_1=E_2$ and a small H_1 in the type I antiferromagnetic phase. (See Fig. 3.) For $\vec{q}$ along [100] there exists a mode with a minimum of energy at X even for small H_1. However, to concentrate the total intensity in this low-energy mode in agreement with experiment, we require a rather sizable H_1. Thus the essential shape of the excitation behavior is determined by the Coqblin-Schrieffer interaction, but the antiferromagnetic Heisenberg interaction H_1 is needed for the fine tuning of the behavior. For $\vec{q}$ along [100], the H_1 interaction causes the intense mode to have flat dispersion close to the Γ point, in addition to shifting the intensity to the lower transverse mode. For $|H_1|>0.4E_1$, the experimental dispersion shape for $\vec{q}$ along [100] is well reproduced. At these values of H_1, the system remains in the type-I phase at all temperatures below the Néel temperature. Assuming an ordering temperature of 25 K as in CeBi, we have scaled the interaction energies for the case of $E_1=E_2$, $H_1=-0.5E_1$, and plotted the experimental results in Fig. 5. The shape of the excitation dispersion given by our model agrees remarkably well with experiment, while the theoretical magnitudes are about 50% too high.

We conclude by summarizing how the present work fits into the context of our understanding of the magnetic behavior of f-electron systems as the f electrons delocalize. The Coqblin-Schrieffer methodology[8] provides a way to treat the behavior of f electrons in the moderately delocalized regime. As derived by Siemann and Cooper,[7] the predominant Coqblin-Schrieffer–type two-ion coupling between the heavier $Ce^{3+}(f^1)$ ions arises from the $m_l=0$ part of the ionic wave function (quantization along the interionic axis), and the resulting interaction explains the equilibrium behavior of CeBi. In this paper, we have shown that the same two-ion interaction can also explain the excitation behavior of CeBi. We conclude that the physics of the magnetic behavior of the Ce monopnictides and monochalcogenides is indeed due to f-electron hybridization with band electrons, and a good physical picture of the hybridization is provided by the Coqblin-Schrieffer treatment.

ACKNOWLEDGMENTS

This research was supported by National Science Foundation Grant No. NSF DMR-82-04261. We are grateful to Dr. J. Rossat-Mignod for keeping us informed about the neutron scattering experiments on CeBi.

*Present address: AT&T Bell Laboratories, Whippany, New Jersey 07981.

[1]B. R. Cooper, J. Magn. Magn. Mater. 29, 230 (1982); D. Yang and B. R. Cooper, in *Crystalline Electric Field Effects in f-electron Magnetism,* edited by R. P. Guertin, W. Suski, and Z. Zolnierek (Plenum, New York, 1982), pp. 381–392.

[2]In addition to the papers cited under Ref. 1, the basic assumptions of the physical picture are also discussed in P. Thayamballi and B. R. Cooper, J. Appl. Phys. 55, 1866 (1984).

[3]J. Rossat-Mignod, P. Burlet, S. Quezel, and O. Vogt, Physica (Utrecht) 102B, 237 (1980).

[4]J. W. Cable and W. C. Koehler, in *Magnetism and Magnetic Materials—1971, Chicago,* Proceedings of the 17th Annual Conference on Magnetism and Magnetic Materials, edited by D. C. Graham and J. J. Rhyne (AIP, New York, 1972), p. 1381.

[5]J. Rossat-Mignod, P. Burlet, J. Villain, H. Bartholin, T. S. Wang, and D. Florence, Phys. Rev. B 16, 440 (1977).

[6]J. Rossat-Mignod, D. Delacote, J. M. Effantin, C. Vettier, and O. Vogt, Physica (Utrecht) 102B, 163 (1983).

[7]R. Seimann and B. R. Cooper, Phys. Rev. Lett. 44, 1015 (1980).

[8]B. Coqblin and J. R. Schrieffer, Phys. Rev. 185, 847 (1969).

[9]D. Yang and B. R. Cooper, J. Appl. Phys. 52, 2234 (1981).